Paaua Science Journal

Paper 17

*PaauaSci.J.***2025**, issue 1, 201-213
DOI: https://doi.org/10.65760/paaujs.v1i1.14

COMPLEXATION-DRIVEN REMOVAL OF Cr(III) AND Pb(II) IONS FROM AQUEOUS MEDIA USING A SCHIFF BASE LIGAND

Mohammed Umar Adaji[1], Alexander David Onoja [1], Samuel Attah Egu[1] Alifa David Jacob [1] Joseph Abiodun Dauda[1], Usman Salifu Oma [1], Clifford Baba Okpanachi[2], Aminu Omale[1], Abdulrahman O. C. Aliyu[1] and Martha D Ekundayo[1]

[1]*Department of Pure and Industrial Chemistry, Kogi State University, Anyigba, Nigeria.*

[2]*Department of Industrial Chemistry, Federal University of Applied Sciences, Kachia, Kaduna State*

**For Corresponding author: Email address: adajimed@gmail.com*

Received 10-05-2026 **Accepted** 15-05-2026 **Published on line** 19-05-2026

Abstract

A Schiff base ligand, (E)-N¹-(2-hydroxybenzylidene)nicotinohydrazide (HNH), was synthesized via the reflux condensation of nicotinic acid hydrazide with salicylaldehyde. The ligand was evaluated for its sorption efficacy in the removal of Cr(III) and Pb(II) ions from aqueous solutions. Systematic studies were conducted to investigate the influence of key parameters, including contact time, solution pH, initial metal ion concentration, and temperature, on the adsorption performance of HNH. The experimental data were fitted to both Langmuir and Freundlich isotherm models, revealing favorable adsorption characteristics under the studied conditions. Thermodynamic analysis indicated that the sorption process was endothermic, with positive enthalpy changes (ΔH) of 115.81 kJmol^{-1} for Cr(III) and 103.37 kJmol^{-1} for Pb(II). Additionally, positive entropy values (ΔS) of 2.67 and 2.42 kJmol^{-1}K^{-1} for Cr(III) and Pb(II), respectively, suggest an increase in randomness at the solid–solution interface. The negative Gibbs free energy values (ΔG) across all temperatures confirm the spontaneous and chemisorptive nature of the sorption process. These findings demonstrate that the HNH ligand is an efficient and thermodynamically favorable adsorbent for the remediation of Cr(III) and Pb(II) ions from contaminated water.

Keywords: Schiff base, Sorption, thermodynamic, Langmuir, Freundlich, Isotherm

Introduction

Industrial wastewater comprises several harmful compounds that endanger human health, aquatic environments, and agriculture. Heavy metals including Cr, Zn, Pb, Cu, Fe, Cd, Ni, As and Hg are significant pollutants derived from industries such as paint, dye, textile, pharmaceutical, paper, and fine chemicals (Wang & Yang, 2016). Additional contaminants comprise phenol and phenolic chemicals (Rajkumar & Palanivelu, 2004). Industrial effluent sources encompass mining, metal finishing, steel manufacturing, industrial laundering, power generation, and oil refining. These discharges generally comprise chemicals, heavy metals, oils, pesticides, medicines, and other wastes (Azimi et al., 2017). The treatment of industrial wastewater is complex due to the necessity for customized solutions for each sector. Adsorption is extensively employed for water filtration owing to its simplicity, cost-effectiveness, and efficacy (Shahraki et al., 2019). Prevalent adsorbents encompass nanoparticles (Varsha et al., 2021) chitosan (Tyagi et al., 2018), organic resins (Zhang & Zhou, 2011), mineral-based materials (Li et al., 2020), carbon nanostructures (Chen et al., 2020), and Schiff bases (Liu et al., 2018; Abdul et al., 2019 Nonetheless, numerous adsorbents are expensive and intricate to produce. Schiff bases are appealing alternatives owing to their economical synthesis and the presence of nitrogen and oxygen donor atoms, which efficiently chelate metals (Zhang et al., 2017). Schiff bases are imine compounds synthesised through the condensation of amines with aldehydes or ketones. Their facile synthesis and many applications in coordination chemistry, industry, and biology render them important ligands. This research examines a Schiff base derived from nicotinic acid hydrazide and salicylaldehyde for the adsorptive elimination of Cr(III) and Pb(II) ions from aqueous solutions.

Experimental Methods

Materials

All chemicals used in this work were of highest grade obtained from Sigma - Aldrich, and they include; Nicotinic acid hydrazide (99 %), Salicyaldehyde (98%), Ethanol (99%), Distilled water (100%), Chromic Sulphate ($Cr_2(SO_4)_3.6H_2O$), Lead Nitrate $Pb(NO_3)_2$, and Hydrochloric Acid (HCl).

Experiments

Preparation of (E)-N1-(2-hydroxybenzylidene)nicotinohydrazide

The synthesis of (E)-N1-(2-hydroxybenzylidene)nicotinohydrazide was carried out following the protocol in our previously described and published articles (Adaji et al., 2022; Adaji et al., 2024) without any modification.

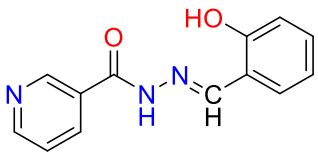

Scheme 1: **(E)-N1-(2-hydroxybenzylidene)nicotinohydrazide**

Characterization

FT-IR spectrum was obtained in the 400 – 4000 cm^{-1} range, by Agilant Technology spectrophotometry. KBr pellets were used for solid samples before and after adsorption.

Batch adsorption process

The adsorption studies were obtained by using the batch method (Li et al., 2015; Dawudu et al., 2014). 0.12g of the Schiff base ligand was suspended in 10.0cm^3 of aqueous solution with cations at several concentrations from 10 – 25mg/L. the samples were mechanically stirred for 2 h at 298 k and the solid was separated by filtration. The influence of adsorption parameters such as contact time (2 – 8h), effect of temperature (308 – 323 K), effect of solution pH (2 - 8) on the adsorptive removal of metal ions was investigated in batch mode. To prepare the stock solution 12.741 g of $Cr_2(SO_4)_3.6H_2O$ (99%) and 1.5985g of $Pb(NO_3)_2$ (98%) were accurately weighed using analytical weighing balance. The weighed amounts were then dissolved in beakers containing distilled water. After complete dissolution they were quantitatively transferred into 1.0 L Volumetric flasks to give 1000 mg/L of the metal salts solutions (stock solution). The content adsorbed was determined by sampling the supernatant, using a UNICAM model 930 flame atomic absorption spectrometer (AAS) after suitable dilution if required. The amounts of cations adsorbed by adsorbent was calculated as

$$q = \frac{(Co-C)V}{w} \qquad (1)$$

Where q is the amount of metal ion adsorbed onto unit amount of the adsorbent ($mmolg^{-1}$), Co and C are the concentrations of metal ions in the initial and equilibrium concentration of the metal ions in aqueous phase (mmoldm-1), V is the volume of the aqueous phase (L), and w is the dry weight of the adsorbent.

Results and Discussions

Effect of Contact Time

The effect of contact time on the adsorptive removal of the metal ions were carefully studies. (Fig. 1) depicts the adsorption of Cr(III) and Pb(II) ions with increasing contact time. At 2 h, the percentage removal of Cr(III)) and Pb(II) was 76.6 % and 72.1 %, respectively. The percentage removal of the metals ion decreased gradually as the time increased up to 8 h, with a decreased in percentage removal of Cr(III)) and Pb(II) to 61.75 % and 60.5 %, respectively. The adsorption process is more efficient at a reduced time of 2–4 h, this may be attributed to the high affinity and interaction between the adsorbent Schiff base and the metal ion due to the availability of a more active site on the Schiff base (Khobragade and Pal, 2015).

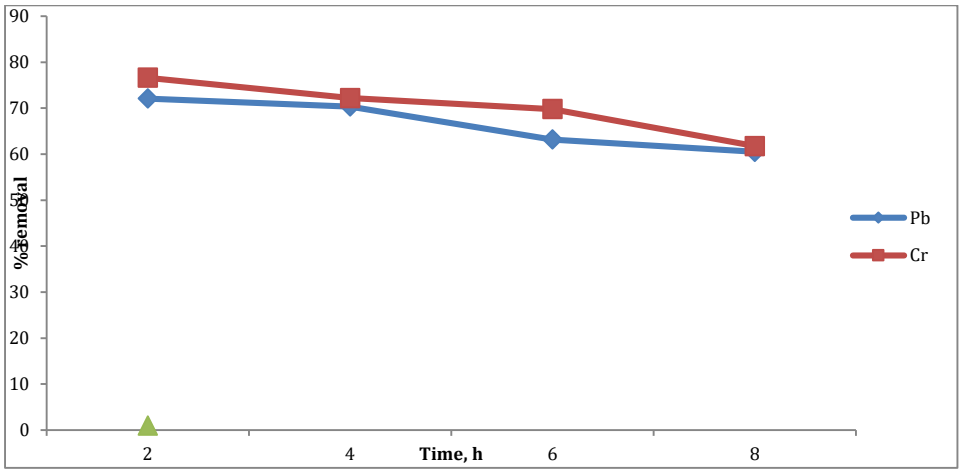

Figure 1: Effect of Time on the adsorption of Cr(III) and Pb(II)

Effect of initial concentration

The effect of the initial concentration of the metal ions on its adsorption onto the prepared adsorbent is presented in Fig. 2. The experiment was carried out at varied concentration of 10 – 25 mg/L at fixed adsorbent dose of 0.12 g, pH = 5, contact time of 45 min and at room temperature in batch mode operation. As shown in Fig. 3, the percentage removal of Cr(III) and Pb(II) decreases with increasing initial concentration of the metal ions. At low initial concetrations, relatively high sorptions were observed as a result of the high ratio of adsorbent surface biniding sites to the heavy metals concentrations, this means that a fewer number of heavy metals ions were competing for the available binding sites on the adsorbent (Bello and Adegoke, 2017; Ravel et al., 2016). Althouh, adsorption capacity, (qe) increases with increasing initial concentration of the heavy metals because as the molecular concentration increases, the chances of collisions between molecule and adsorbent surface increase due to increase in mass transfer from solution phase to solid phase (Shuka and Vankar, 2012). In this study it was found that as the concentrations of the metal ions increases from 10 to 25 mg/L, there was an increase in adsorption capacity from 0.443 to 1. 565 mg/g and 0.4925 to 1. 623 mg/g for Cr and Pb ions respectively. This increase in the adsorption capacity with increase in the initial concentratration is additional evidence that the adsorption process was efficient.

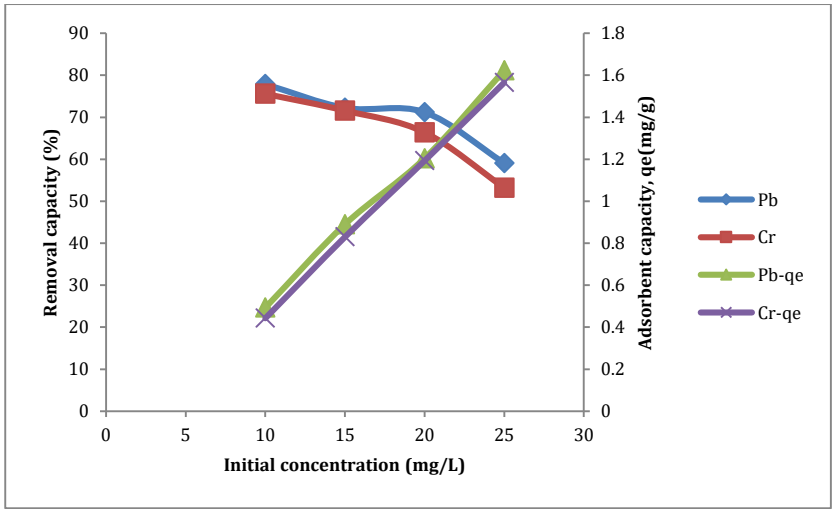

Figure 2: **Effect of initial concentration on the adsorption of Cr(III) and Pb(II)**

Effect of solution pH

The solution pH can affect the surface charge of the adsorbent, the degree of ionization of the different pollutants, the dissociation of functional groups on the active sites on the adsorbent, as well as the structure of the Schiff base ligand (Raval et al., 2016).

The adsorption efficiency increased with increasing pH from 2 to 6 for both Pb and Cr ions. At low pH, adsorption was suppressed due to active sites and competition between H^+ ions and metal ions for adsorption sites. As the pH increased, deprotanation of the donor atoms enhanced metal – ligand coordination, resulting in improved adsorption efficiency. Maximum adsorption was observed at pH 6, indicating favorable interactilon between the metal ions and the Schiff base functional groups. Higher adsorption of Cr compared to Pb suggests stronger affinity of chromium ions toward the adsorbent surface. pH values above 6 were avoided to prevent metal hydroxide precipitation. This result is in agreement with other findings elsewhere (Hosseini et al., 2024)

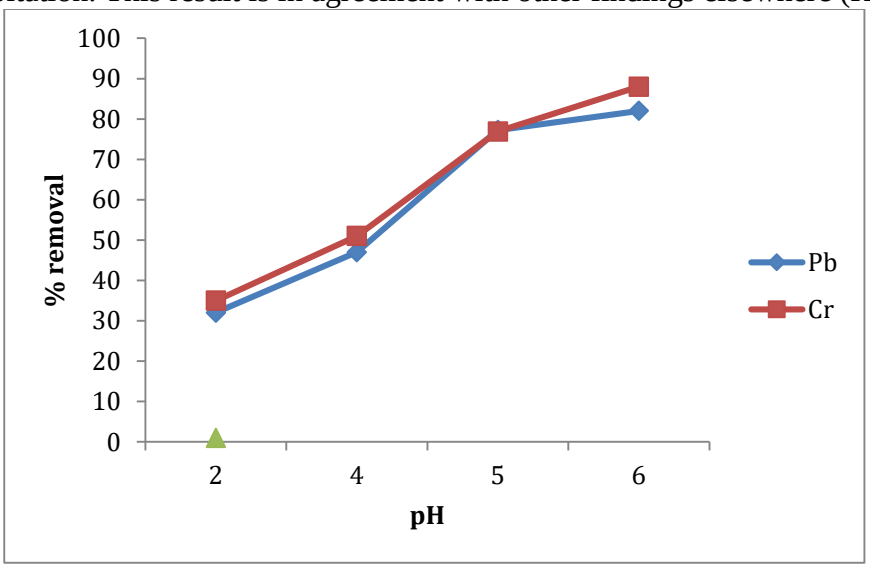

Figure 3: **Effect of pH on the adsorption of Cr(III) and Pb(II)**

Effect of Temperature and Adsorption Thermodynamic

Temperature, like other chemical reaction processes, has a significant impact on adsorption processes. The rate of diffusion of adsorbate molecules across the external boundary layer and internal pores of adsorbent particles increases as temperature rises. The sorption of Cr and Pb onto the Schiff base ligand revealed that heavy metal adsorption increases with increasing temperature from 308 K to 323 K (Fig. 4). At the maximum temperature of 323 k, the percentage removal for Cr(III) and Pb(II) was 80.2% and 78.7%, respectively, representing nearly 100 % removal efficiency. The increase in Cr(III) and Pb(II) adsorption by the Schiff base with increasing temperature indicates that the adsorption process is exothermic, this is in agreement with findings made by (Hosseini et al., 2024)

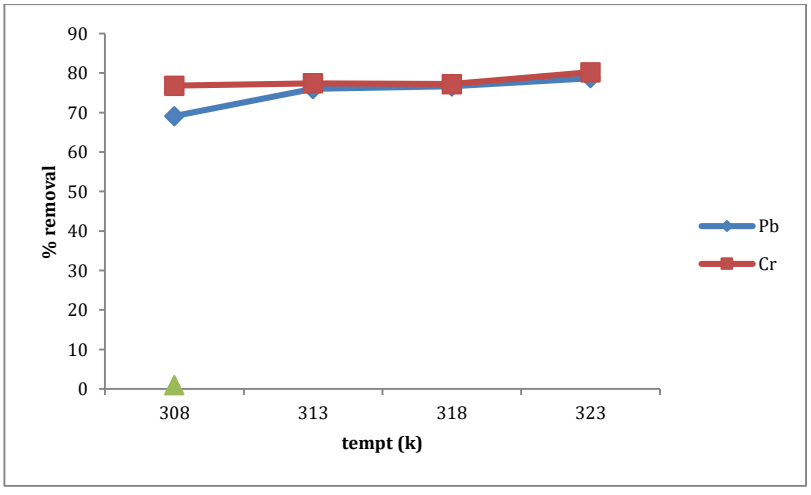

Figure 4: **Effect of temperature on adsorption of Cr(III) and Pb(II)**

Adsorption Isotherm

Cr^{3+} and Pb^{2+} adsorption by Schiff base ligand were analyzed using Langmuir and Freundlich Isotherms. The Langmuir isotherm is used to characterize the monolayer adsorption, which is represented by the following linear form:

$$\frac{Ce}{qe} = \frac{1}{qmaxb} \quad (2)$$

The essential characteristic of the Langmuir isotherm is expressed in terms of a dimensionless constant separation factor, RL, which is defined as;

$$Rl = \frac{1}{1 + bCm} \quad (3)$$

Where, qe is the equilibrium adsorption uptake of the adsorptive metals ions.
The Langmuir isotherm is a plot of Ce/qe (y-axis) against Ce (x-axis) (Fig 5a &5b) where 1/QmLc is the intercept and 1/Qm is the slope (gradient), Qm is the maximum adsorption capacity with single layer presentation (mg/g), Lc is the Langmuir constant (L/mg). The Freundlich isotherm is generally applicable to the adsorption occurred on heterogeneous surface. The linear form is shown:

$$\text{Log } q_e = \log K_f + 1/n \log C_e \quad (4)$$

The Freundlich isotherm is a plot of log qe (y-axis) against log Ce (x-axis) (Fig. 6a & 6b) where Kf is the slope, associated with adsorption capacity, n is isotherm constant associated with adsorption intensity.

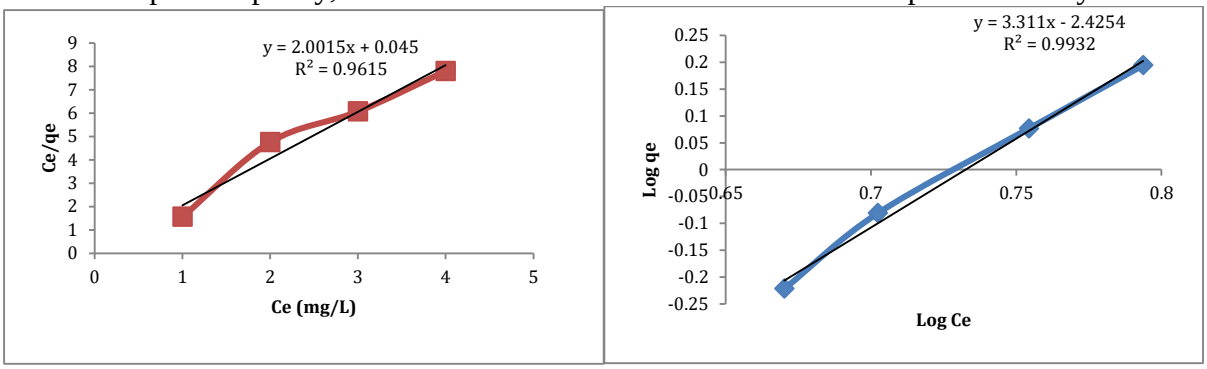

Figure 5a: **Langmuir Isotherm for Cr and Figure 6b: Freundlich Isotherm for Cr**

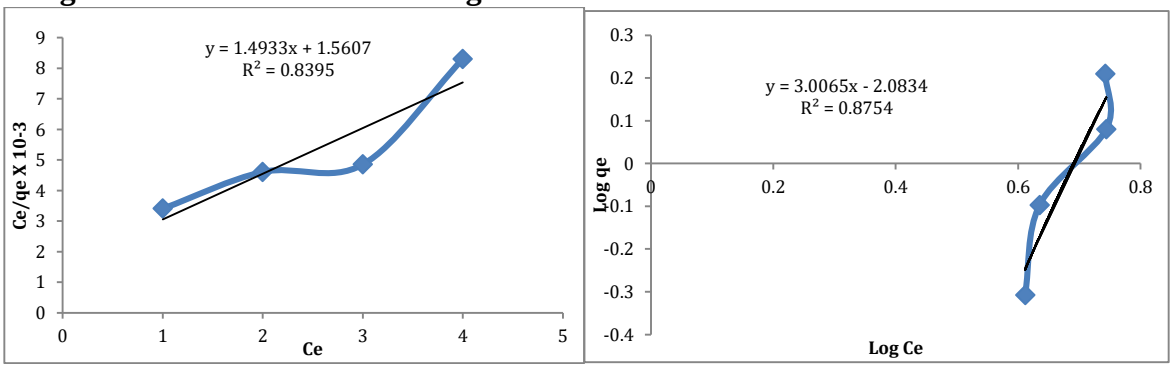

Figure 5b: **Langmuir Isotherm for Pb and** Figure 6b: **Freundlich Isotherm for Pb**

Adsorption Isotherm

Cr^{3+} and Pb^{2+} adsorption by Schiff base ligand were analyzed using Langmuir and Freundlich Isotherms. The Langmuir isotherm is used to characterize the monolayer adsorption, which is represented by the following linear form:

$$\frac{Ce}{qe} = \frac{1}{qmaxb} \quad (2)$$

The essential characteristic of the Langmuir isotherm is expressed in terms of a dimensionless constant separation factor, RL, which is defined as;

$$Rl = \frac{1}{1 + bCm} \quad (3)$$

Where, qe is the equilibrium adsorption uptake of the adsorptive metals ions.
The Langmuir isotherm is a plot of Ce/qe (y-axis) against Ce (x-axis) (Fig 5a &5b) where 1/QmLc is the intercept and 1/Qm is the slope (gradient), Qm is the maximum adsorption capacity with single layer

presentation (mg/g), Lc is the Langmuir constant (L/mg). The Freundlich isotherm is generally applicable to the adsorption occurred on heterogeneous surface. The linear form is shown:

$$\text{Log } q_e = \log K_f + 1/n \log C_e \quad (4)$$

The Freundlich isotherm is a plot of log qe (y-axis) against log Ce (x-axis) (Fig. 6a & 6b) where Kf is the slope, associated with adsorption capacity, n is isotherm constant associated with adsorption intensity.

Equilibrium Isotherm Studies

Adsorption Isotherm describes how the adsorbate interacts with the adsorbent and provides a comprehensive understanding of the nature of the interaction. Isotherms help to provide information about the optimum use of adsorbents (Deng et al., 2011). Isotherms curves are extremely relevant for adsorption purposes since it provides information about the interaction mechanisms and maximum adsorption capacity of a determined adsorbent (Mohrazi & Ghasemi-Fasaei, 2023). To determine the best–fit biosorption isotherm model, the equilibrium data were analyzed by the most common isotherm models such as the Langmuir and Freundlich Isotherm models. These models were helpful to determine the maximum adsorption capacity of adsorbate for the given adsorbent. They differ in the basic assumptions, the shape of the isotherm, and the nature of the adsorbent surface. The Freundlich isotherm is derived by assuming a heterogeneous surface with a non–uniform distribution of heat of adsorption over the surface. Whereas, in Langmuir's theory, the basic assumption is that the sorption takes place at specific homogenous sites within the adsorbent (Astar et al., 2021). The mathematical expressions for those isotherms were presented in Equation 5.

$$\frac{Ce}{qe} = \frac{1}{kLqm} + \frac{Ce}{qm} \quad (5)$$

$$logqe = logkf + \frac{logCe}{n} \quad (6)$$

Where Ce is the equilibrium concentration of solute (mgL^{-1}), qe is the amount of solute adsorbed per unit weight of adsorbent ($mg\ g^{-1}$), qm is the adsorption capacity ($mg\ g^{-1}$) or monolayer capacity, and KL is the Langmuir constant related to the energy of adsorption (Lmg^{-1}), Kf and n are empirical constants for Freundlich isotherm incorporating all parameters affecting the adsorption process such as sorption capacity and sorption intensity respectively. The isotherm curves were drawn Ce/qe versus Ce for Langmuir isotherm and logqe vs log Ce graph for Freundlich isotherm model and presented in (Fig. 5a and 6a) respectively. The isotherm parameters such as qm and kL for the Langmuir isotherm model can be calculated from the intercept and the slope of Ce/qe versus Ce graph respectively. The value of KF and n for Freundlich can be calculated from logqe vs logCe graph. All the isotherm parameters calculated from the graph and correlation factor (R_2) for both models were presented in Table 1. As shown in the table the collation factor for Langmuir (R_2= 0.9615) for Cr and (R2 = 0.8395) for Pb were close to 1 confirms Langmuir isotherm model better describes the interaction between the adsorbent and adsorbate in the aqueous system. The efficiency of the Langmuir adsorption process could be predicted by the dimensionless equilibrium parameter RL, which is defined by the following equation 7 (Kumar & Laskar, 2019)

$$RL = \frac{1}{1+KLCo} \quad (7)$$

Where kL is the Langmuir constant related to the energy of adsorption (Lmg^{-1}) and Co is the initial concentration (mgL^{-1}). The calculated RL values at different initial adsorbent concentrations were presented in Table 2. RL values indicate the adsorption nature to either unfavourable if (RL>1), linear if (RL= 1), favourable if 0 <RL<1 and irreversible if RL = 0 (Mohrazi & Ghasemi-Fasaei, 2023). For this study, all the values lie between 0 and 1 confirming that the adsorption of the metals onto the Schiff base adsorbent was favourable.

The sorption data were also compared by the Freundlich equation in the following form

$$qe = K_F Ce^{1/n} \quad 8$$

and a linear form of the Freundlich equation is

$$ln\ ln\ q_{e=}\ ln\ ln\ K_F \quad 1/\text{n ln } C_e \quad 9$$

Where, qe is the equilibrium solute concentration on adsorbent (mg/g), Ce is the equilibrium concentration of the solute (mg/g). Kf is the Freundlich constant (mmol g^{-1}) which indicates the sorption capacity and represents the strength of the absorptive bond, and n is the heterogeneity factor which represents the bond distribution. The plot of logqe vs logCe is a straight line for the two cations. The sorption data obey the Freundlich isotherm as well. The values of Kf and n can be calculated from the intercept and slope of the plot shown in (Fig. 5b & 6b) and the values are presented in Table 1.

For the Freundlich-type adsorption process, the magnitude of the component 'n' gives an indication of the favourability of adsorption capacity. For this study the n value is 3.311 and 3.0065 for Cr and Pb respectively, confirming that the adsorption of the metals is favourable. 1/n indicates the adsorption intensity of metal ions onto the adsorbent becoming more heterogeneous as its value gets closer to 0. The values of 1/n below 1 indicate a normal Freundlich isotherm, while 1/n above 1 indicates cooperative adsorption. Hence, it is observed that our 1/n values were found to be 0.3020 for Cr-HNH and 0.3326 for Pb-HNH were favourable to the model. This result is in agreement with findings obtained elsewhere (Li et al., 2013). The Isotherm constant KF and n were calculated from the linear form of the model, the correlation factor R_2 and KF value are given in Table 1. The values of Freundlich constants Kf and n give a measure of the sorption intensity and capacity of the sorbent, respectively (Khorshidi & Khalaji, 2024).

Adsorption Thermodynamic

The adsorption thermodynamics study of Cr and Pb were studied by calculating Standard Gibb's Free Energy (ΔG). The slope and intercept of the plot of lnKd against 1/T were used to infer Standard Enthalpy (ΔHo) and Standard Entropy and lnKd(ΔSo) respectively as seen in Figure 8. Thermodynamics parameters are not only used to predict the feasibility of a chemical reaction, but they also provide information as to whether the process is endothermic, exothermic, or at equilibrium (Zhu et al., 2023). The negative values of ΔG and positive values of ΔS which determine the disorderliness of the adsorption of solid-liquid interface and the driving force of the reaction is a clear indication that the adsorption of these metal ions by Schiff base is feasible (Li et al, 2021)

If the ΔG < 0 (negative), it indicates that the adsorption occurs spontaneously without the need for external energy. If ΔG > 0 (positive), it means the adsorption does not take place spontaneously and the reaction mechanism needs a supportive force, i.e heat energy.

The calculative ΔG values were negative ranging from -709.495, -749.688 for Cr(III) and -642.269 to -678.583 J/mol for Pb(II) as the temperature increased from 308K to 323K as seen in Table 3 which shows that the adsorption process is chemisorption, also, a confirmation that the process occurs spontaneously. According to (Liu et al., 2021), the principal test for distinguishing chemisorption from physisorption is the magnitude of ΔG values less negative than -25kj/mol are normally considered as signifying physisorption and value more negative than about -40kj/mol are taking to represent chemisorption. The ΔH values of the adsorption process were 115.814 J/mol for Cr(III) and 103.376 J/mol for Pb(II). The positive value is an indication that the adsorption process of the metal ions is endothermic in nature and takes place through chemisorption. The entropy (ΔS) values of 2.679 for Cr(III) ion and 2.421 for Pb(II) ion is an indication that the adsorption process is spontaneous.

These parameters can be calculated using the following relations;

$$\Delta G = \Delta H - T\Delta S \quad (4)$$

$$\Delta G^o = -RT\, lnK_d \quad (5)$$

$$ln\ ln\ Kd = \frac{\Delta H}{RT} + \frac{T\Delta S}{R} \quad (6)$$

$$Where,\ Kd = \frac{qe}{Ce} \quad (7)$$

Where k is equilibrium constant, T absolute temperature in Kelvin, and R is universal gas constant (8.314J/mol/k). By plotting a graph of lnKd versus 1/T Fig 8, the values ΔHo and ΔSo were estimated from the slope and intercept, respectively.

Table 1: Isotherm Parameters Calculated from the Graphs

Isotherm		Cr	Pb
Langmuir	R^2	0.9615	0.8395
	K_L	44.48	0.9569
	$R_L(Lmg^{-1})$	0.00112	0.0496
	q_m(mg/g)	0.4996	0.6696
Freundlich	R^2	0.9932	0.8754
	N	3.311	3.0065
	1/n	0.3020	0.3326
	K_f (L/mg)	266.317	121.171

Table 2: Dimensionless Constant Separation Factor (RL) value at Different Initial Concentration

Adsorbent	R_L values **Concentration mgL^{-1}**			
	0.10	0.15	0.20	0.25
Cr	0.00224	0.00149	0.00112	0.00089
Pb	0.09461	0.06513	0.0496	0.04012

Removal Thermodynamic

The removal thermodynamics study of Cr and Pb were studied by calculating Standard Gibb's Free Energy (ΔG). The slope and intercept of the plot of lnKd against 1/T were used to infer Standard Enthalpy (ΔHo) and Standard Entropy and lnKd(ΔSo) respectively as seen in Figure 7. Thermodynamics parameters are not only used to predict the feasibility of a chemical reaction, but they also provide hinformation as to whether the process is endothermic, exothermic, or at equilibrium (Zhu et al., 2023). The negative values of ΔG and positive values of ΔS which determine the disorderliness of the adsorption of solid-liquid interface and the driving force of the reaction is a clear indication that the adsorption of these metal ions by Schiff base is feasible (Li et al, 2021).

If the ΔG < 0 (negative), it indicates that the adsorption occurs spontaneously without the need for external energy. If ΔG > 0 (positive), it means the adsorption does not take place spontaneously and the reaction mechanism needs a supportive force, i.e heat energy.

The calculative ΔG values were negative ranging from -709.495, -749.688 for Cr(III) and -642.269 to -678.583 J/mol for Pb(II) as the temperature increased from 308K to 323K as seen in Table 3 which shows that the adsorption process is chemisorption, also, a confirmation that the process occurs spontaneously. According to (Liu et al., 2021), the principal test for distinguishing chemisorption from physisorption is the magnitude of ΔG values less negative than -25kj/mol are normally considered as signifying physisorption and value more negative than about -40kj/mol are taking to represent chemisorption. The ΔH values of the adsorption process were 115.814 J/mol for Cr(III) and 103.376 J/mol for Pb(II). The positive value is an indication that the adsorption process of the metal ions is endothermic in nature and takes place through chemisorption. The entropy (ΔS) values of 2.679 for Cr(III) ion and 2.421 for Pb(II) ion is an indication that the adsorption process is spontaneous.

These parameters can be calculated using the following relations;

$$\Delta G = \Delta H - T\Delta S \quad (4)$$

$$\Delta G^o = -RT\, lnK_d \quad (5)$$

$$ln\ ln\ Kd = \frac{\Delta H}{RT} + \frac{T\Delta S}{R} \quad (6)$$

$$Where,\ Kd = \frac{qe}{Ce} \quad (7)$$

Where k is equilibrium constant, T absolute temperature in Kelvin, and R is universal gas constant (8.314J/mol/k). By plotting a graph of lnKd versus 1/T Fig 8,the vales ΔHo and ΔSo were estimated from the slope and intercept, respectively.

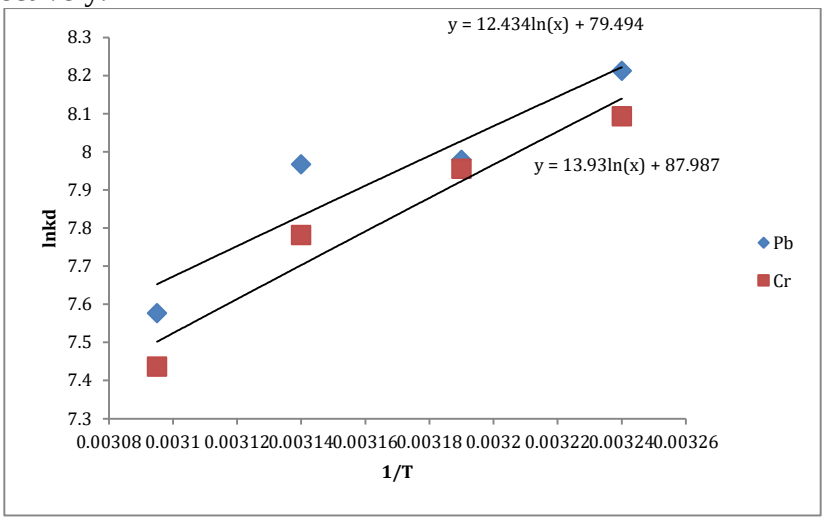

Figure 7: **Plot of lnkd VS 1/T for thermodynamics**

Table 3: **Thermodynamic Parameters for the Adsorption of Metal ions on Adsorbent**

Metal	ΔH° (kJ mol^{-1})	ΔS° (J mol^{-1} K^{-1})	T (k)	ΔG° (kJ mol^{-1})
Cr	115.81	2.67	308	-709.49
			313	-722.89
			318	-736.29
			323	-749.68
Pb	103.37	2.42	308	-642.26
			313	-654.37
			318	-666.47
			323	-678.58

Fourier Transform Infrared (FT-IR) Characterization

The structural changes in the Schiff base ligand before and during the adsorption of Cr(III) and Pb(II) ions from aqueous solutions were evaluated using FTIR spectroscopy. The interaction between the metal ions and the adsorbent's functional groups during the adsorption process was conclusively demonstrated by the spectrum shifts and the appearance or lack of characteristic bands as shown in Table 4. The C=N stretching vibration (azomethine group) was identified as the cause of a notable absorption band in the spectrum of the unmodified Schiff base at 1614 cm^{-1}. This band shifted to 1595 cm^{-1} for Cr(III) and 1602 cm^{-1} for Pb(II) after metal adsorption. These modifications show that the azomethine group was involved in the surface interaction or binding with the adsorbed metal ions. The decrease in frequency could be the consequence of a reduced bond order, which would indicate that the imine's nitrogen atom donated electrons to the adsorbed species on the Schiff base surface, confirming the group's active participation in adsorption. After both metal ions were adsorbed, the N–H stretching vibration, which was initially 3476 cm^{-1}, changed to 3429 cm^{-1}. This change indicates dipole interactions or hydrogen bonding with the adsorbate, which may change the N-H bond's vibrational energy and suggest participation in the adsorption process. The phenolic -OH group's involvement in the metal-binding mechanism is demonstrated by the absence of the O-H stretching band at 3141 cm^{-1} upon adsorption. This could be explained by surface complexation of the phenolic oxygen with the adsorbed Cr(VI) and Pb(II) ions, hydrogen bonding, or ion-dipole interactions. The deprotonation of the -OH group and its subsequent interaction with the metal ions are indicated by the absence of this peak. While the appearance of a prominent band at 872 cm^{-1} in both spectra suggests metal–oxygen (M–O) surface interaction, new absorption bands observed at 760 cm^{-1} (Cr) and 700 cm^{-1} (Pb) are suggestive of metal–nitrogen (M–N) interactions as

shown in scheme 2. These features further confirm that the Schiff base ligand has functional moieties on its surface that can bind metal ions through physisorption and/or chemisorption processes. The C–N (aromatic amine) stretching band showed a notable shift from 1268 cm^{-1} to 1200 cm^{-1}, supporting the idea that the adsorption of Cr(III) and Pb(II) altered the local electronic environment of nitrogen. From 1357 cm^{-1} to 1364 cm^{-1}, the C–O stretching band shifted, indicating possible interactions or proximity effects between the oxygen atom in the C–O group and the metal ions. These FTIR findings provide strong proof that Cr(III and Pb(II)) bind adsorptively to the Schiff base ligand. Active functional groups like C=N, O–H, N–H, C–O, and aromatic nitrogen are thought to improve the adsorption process. These groups function as adsorption sites through processes like surface coordination, ion exchange, hydrogen bonding, and electrostatic contact. These results validate the Schiff base's efficacy and adaptability as an adsorbent for heavy metal removal from aqueous solutions (Liu et al., 2018).

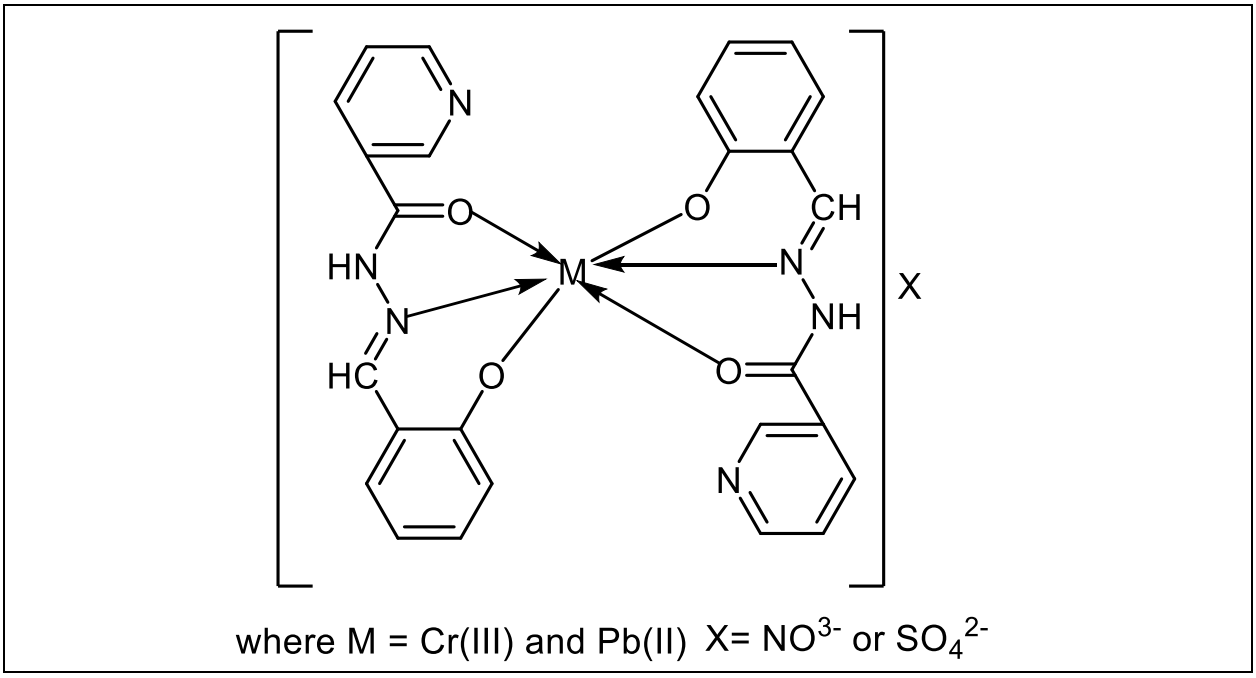

Scheme 2: **Metal – Ligand Complexation Mechnism**

Table 4: **FTIR Spectra Changes of the Schiff base after Chelation with Pb(II) and Cr(III) ions**

Schiff base (cm^{-1})			**Functional groups**
Before adsorption	**After adsorption**		
	Cr	**Pb**	
1614	**1595**	**1602**	**C=N (Imine or azomethine)**
3476	**3429**	**3429**	**N-H**
-	**760**	**700**	**M-N**
-	**872**	**872**	**M-O**
1268	**1200**	**1200**	**C-N (aromatic)**
3141	**-**	**-**	**OH**
1357	**1364**	**1364**	**C-O**

Conclusions

In this study, a Schiff base ligand, (E)-N^1-(2-hydroxybenzylidene)nicotinohydrazide (HNH), was successfully synthesized from nicotinic acid hydrazide and salicylaldehyde and investigated for its interaction with Cr(III) and Pb(II) ions in aqueous medium. The results demonstrated that the efficiency of metal ion removal increased with increasing contact time, temperature, pH, and initial metal ion concentration, indicating enhanced metal–

ligand interaction under favourable experimental conditions.The experimental findings revealed that the Schiff base ligand possesses active donor sites, particularly the azomethine nitrogen and phenolic oxygen atoms, which play significant roles in the coordination and sequestration of the metal ions. Thermodynamic studies indicated that the process was spontaneous and endothermic in nature, while the low activation energy and other physicochemical parameters suggested that the interaction proceeded predominantly through a physical coordination mechanism. Furthermore, spectroscopic analyses confirmed the involvement of the functional groups in the binding process through noticeable shifts and changes in characteristic absorption bands after interaction with the metal ions. The study therefore establishes the synthesized Schiff base ligand as an effective chelating agent for Cr(III) and Pb(II) ions in aqueous systems. The work highlights the promising potential of Schiff base ligands in heavy metal ion remediation and provides valuable insight into their coordination behaviour, opening opportunities for further modification and immobilization toward practical environmental applications.

Supplementary Material

Not applicable.

References

Abdul, S., Muhammad, A. S., Ibrahim, M. A., & Ibrahim, M. B. (2019). Thermodynamic study on the adsorptive removal of Cr(VI) and Ni(II) metal ions using Schiff base as adsorbent. *Moroccan Journal of Chemistry, 7*(3), 506–515.

Adaji, M. U., Iorungwa, M. S., & Salawu, O. W. (2024). Characterization of Schiff base ligand and its metal complexes. In *Novelties in Schiff Bases* (1st ed., pp. 1–32).

Adaji, M. U., Wuana, R. A., Itodo, A. U., Eneji, I. S., & Iorungwa, M. S. (2022). Metal complexes of (E)-N¹-(2-hydroxybenzylidene)nicotinohydrazide Schiff base: Synthesis, characterization and nematicidal activity. *Arabian Journal of Chemical and Environmental Research, 8*(2), 418–435.

Ajenifuja, E., Ajao, J., & Ajayi, E. (2017). Adsorption isotherm studies of Cu(II) and Co(II) in high concentration aqueous solutions on photocatalytically modified diatomaceous ceramic adsorbents. *Applied Water Science, 7*, 3793–3801.

Astar, F. S., Kukwa, D. T., Wuana, R. A., & Arwenyo, B. (2021). Kinetics and thermodynamic studies: Adsorption of Pb, Cr and Ni ions from spent lubrication oil using acid modified clay. *American Journal of Analytical Chemistry, 12*, 109–120.

Azimi, A., Azari, A., Rezakazemi, M., & Ansarpour, M. (2017). Removal of heavy metals from industrial wastewaters: A review. *ChemBioEng Reviews, 4*(1), 37–59.

Bello, O. S., Adegoke, K. A., & Akinyunni, O. O. (2017). Preparation and characterization of a novel adsorbent from *Moringa oleifera* leaf. *Applied Water Science, 7*, 1295–1305.

Chen, T., Zhang, S., & Yuan, Z. (2020). Adsorption of solid organic waste composting products: A critical review. *Journal of Cleaner Production, 272*, 122712.

Dawodu, F. A., & Akpomie, K. G. (2014). Simultaneous adsorption of Ni(II) and Mn(II) ions from aqueous solution onto a Nigerian kaolinite clay. *Journal of Materials Research and Technology, 3*(2), 129–141.

Deng, H., Lu, J., Li, G., Zhang, G., & Wang, X. (2011). Adsorption of methylene blue on adsorbent materials produced from cotton stalk. *Chemical Engineering Journal*, *172*, 326–334. https://doi.org/10.1016/j.cej.2011.06.013

Fu, F. L., & Wang, Q. (2011). Removal of heavy metal ions from wastewater: A review. *Journal of Environmental Management*, *92*, 407–418. https://doi.org/10.1016/j.jenvman.2010.11.011

Hassan, R., Abdul Latif, N., Montasser, M., & Abdul-Kader, A. H. (2015). Adsorption of Ni(II) and Fe(II) ion using cross-linked modified chitosan–khellinone Schiff base for wastewater treatment. *Environmental Science, Chemistry*, *4*(6), 4910–4916.

Hosseini, S., Khalaji, A. D., Mokhtari, A., & Kevanfard, M. (2024). Adsorption study of eosin yellow and fluorescein dyes from aqueous solution using chitosan Schiff base/polyvinyl acetate and its Fe2O3 nanocomposite. *Cellulose*, *31*, 5281–5295. https://doi.org/10.1007/s10570-024-05836-6

Khobragade, M. U., & Pal, A. (2015). Adsorptive removal of Cu(II) and Ni(II) from single metal, binary metal and industrial wastewater systems by surfactant modified alumina. *Journal of Environmental Science and Health, Part A, Toxic/Hazardous Substances and Environmental Engineering*, *50*(4), 385–395. http://dx.doi.org/10.1080/10934529.2015.987535

Kumar, R., Laskar, M. A., & Hewaidy, I. F. (2019). Modified adsorbents for removal of heavy metals from aqueous environment: A review. *Earth Systems and Environment*, *3*, 83–93. https://doi.org/10.1007/s41748-018-0085-3

Leechart, P., Nakbanpote, W., & Thiravetyan, P. (2009). Application of 'waste' wood-shaving bottom ash for adsorption of azo reactive dye. *Journal of Environmental Management*, *90*, 912–920. https://doi.org/10.1016/j.jenvman.2008.02.005

Li, Y., Du, Q., Liu, T., Peng, X., Wang, J., Sun, J., Wang, Y., Wu, S., Wang, Z., & Xia, Y. (2013). Comparative study of methylene blue dye adsorption onto activated carbon, graphene oxide, and carbon nanotubes. *Chemical Engineering Research and Design*, *91*, 361–368. http://dx.doi.org/10.1016/j.cherd.2012.07.007

Li, D., Li, J., Dong, H., Li, X., Zhong, J., Ramaswamy, S., & Xu, F. (2021). Pectin in biomedical and drug delivery applications: A review. *International Journal of Biological Macromolecules*, *185*(8), 49–65. https://doi.org/10.1016/j.ijbiomac.2021.06.088

Li, Q., Li, X., & Sun, J. (2020). Removal of organic and inorganic matters from secondary effluent using resin adsorption and reuse of desorption eluate using ozone oxidation. *Chemosphere*, *251*, 126442. https://doi.org/10.1016/j.chemosphere.2020.126442

Li, X., Chen, S., Fan, X., Quan, X., Tan, F., Zhang, Y., & Gao, J. (2015). Adsorption of ciprofloxacin, bisphenol and 2-chlorofloxacin on electrospun carbon nanofibres in comparison with powder activated carbon. *Journal of Colloid and Interface Science*, *447*, 120–127. https://doi.org/10.1016/j.jcis.2015.01.042

Lima, H. H., Maniezzo, R. S., Llop, M. E., Kupfer, V. L., Arroyo, P. A., Guilherme, M. R., Rubira, A. F., Girotto, E. M., & Rinaldi, A. W. (2019). Synthesis and characterization of pecan nutshell-based adsorbent with high specific area and high methylene blue adsorption capacity. *Journal of Molecular Liquids*, *276*, 570–576. https://doi.org/10.1016/j.molliq.2018.12.010

Liu, X., He, C., Yu, X., Bai, Y., Ye, L., Wang, B., & Zhang, L. (2018). Net-like porous activated carbon materials from shrimp shell by solution-processed carbonization and H3PO4 activation for methylene blue adsorption. *Powder Technology*, *326*, 181–189. https://doi.org/10.1016/j.powtec.2017.12.034

Liu, X., Li, M., & Singh, S. K. (2021). Manganese-modified lignin biochar as adsorbent for removal of methylene blue. *Journal of Materials Research and Technology*, *12*, 1434–1445. https://doi.org/10.1016/j.jmrt.2021.03.076

Mahdi, A. M., & Guzar, S. H. (2024). Synthesis, characterization and spectral studies of Cu(II) with a new ligand 5-[{3-[(2-carbamothioylhydrazinylidene)methyl]-4-hydroxyphenyl}diazenyl]-2-hydroxybenzoic acid. *Moroccan Journal of Chemistry*, *12*(3), 1058–1072. https://doi.org/10.48317/IMIST.PRSM/morjchem-v12i3.46918

Mohrazi, A., & Ghasemi-Fasaei, R. (2023). Removal of methylene blue dye from aqueous solution using an efficient chitosan-pectin bio-adsorbent: Kinetics and isotherm studies. *Environmental Monitoring and Assessment*, *195*(2), 339. https://doi.org/10.1007/s10661-022-10900-4

Rajkumar, D., & Palanivelu, K. (2004). Electrochemical treatment of industrial wastewater. *Journal of Hazardous Materials*, *113*, 123–129. https://doi.org/10.1016/j.jhazmat.2004.05.039

Raval, N. P., Shah, P. U., & Shah, N. K. (2016). Nanoparticles loaded biopolymer as effective adsorbent for adsorptive removal of malachite green from aqueous solution. *Water Conservation Science and Engineering*, *1*, 69–81. https://doi.org/10.1007/s41101-016-0004-0

Saad, A. A. (2010). Removal of heavy metals from industrial water by adsorption. *Trends in Applied Science Research, 5*, 138–145. https://doi.org/10.1016/j.jwpe.2017.12.005

Shahraki, S., Delarami, H. S., & Khosravi, F. (2019). Synthesis and characterization of an adsorptive Schiff base–Chitosan nanocomposite for removal of Pb(II) ion from aqueous media. *International Journal of Biological Macromolecules, 139*, 577–586. https://doi.org/10.1016/j.ijbiomac.2019.07.223

Tyagi, S., Rawtani, D., Khatri, N., & Tharmavaram, M. (2018). Strategies for nitrate removal from aqueous environment using nanotechnology: A review. *Journal of Water Process Engineering*, *21*, 84–95. https://doi.org/10.1016/j.jwpe.2017.12.005

Vankar, P. S., & Shukla, D. (2012). Biosynthesis of silver nanoparticles using lemon leaves extract and its application for antimicrobial finish on fabric. *Applied Nanoscience, 2*, 163–168. https://doi.org/10.1007/s13204-011-0051-y

Varsha, M., Kumar, P. S., & Rathi, B. S. (2021). A review on recent trends in the removal of emerging contaminants from aquatic environment using low-cost adsorbents. *Chemosphere, 287*, 132270. http://dx.doi.org/10.1016/j.chemosphere.2021.132270

Wang, Q., & Yang, Z. (2016). Industrial water pollution, water environment treatment, and health risks in China. *Environmental Pollution, 218*, 318–365. https://doi.org/10.1016/j.envpol.2016.07.011

Zhang, J., & Zhou, L. O. U. (2011). Kinetic, isotherm and thermodynamic studies of the adsorption of methyl orange from aqueous solution by Chitosan/alumina composite. *Journal of Chemical Engineering Data, 457*, 412–419. http://dx.doi.org/10.1021/je2009945

Zhang, H., Chen, C., & Gray, E. M. (2017). Effect of feedstock and pyrolysis temperature on properties of biochar governing end use efficacy. *Biomass and Bioenergy, 105*, 136–146. https://doi.org/10.1016/j.biombioe.2017.06.024

X

